Check for updates

Structural properties of a new class of stellar structures in modified teleparallel gravity

Aylin Caliskan[1], Rana Muhammad Zulqarnain[2]*, Ertan Güdekli[3], Imran Siddique[4], Hijaz Ahmad[5,6,7] and Sameh Askar[8]

[1]Graduate School of Engineering and Science, Istanbul University, Istanbul, Türkiye, [2]School of Mathematical Sciences, Zhejiang Normal University, Jinhua, Zhejiang, China, [3]Department of Physics, Istanbul University, Istanbul, Türkiye, [4]Department of Mathematics, University of Management and Technology, Lahore, Pakistan, [5]Section of Mathematics, International Telematic University Uninettuno, Roma, Italy, [6]Department of Computer Science and Mathematics, Lebanese American University, Beirut, Lebanon, [7]Operational Research Center in Healthcare, Near East University, Nicosia, Cyprus, [8]Department of Statistics and Operations Research, College of Science, King Saud University, Riyadh, Saudi Arabia

This paper explores new neutron star models based on spherically symmetric space−time. We take into account the gravitational effects of $f(T, \mathcal{T})$ gravity, in which T is the torsion and $\mathcal{T}$ is the trace of the energy−momentum tensor. Field equations are evaluated by incorporating the off-diagonal tetrad. In this paper, we discuss the detailed properties of compact star candidates 4U1538−52, J0437−4,715, J0030 + 0451, and 4U1820−30, like energy density, pressure profiles, gradients, anisotropy, energy conditions, equation of state, speeds of sound, TOV equation, and compactification parameters. We discuss all these characteristics using the quadratic cosmological model of $f(T, \mathcal{T})$ gravity. We use the well-famed junction equations to evaluate the unknown parameters. Our detailed and comprehensive graphical analysis ensures that the model containing the anisotropic nature of stellar structures is physically acceptable, regular, and stable.

KEYWORDS

gravitation, cosmology, modified gravity, f(T) gravity, f(T, T) gravity, f(R) gravity

1 Introduction

The expansion of the Universe first came into discussion in 1998 (Riess et al., 1998). This knowledge was genuinely adverse to the expectations of observers. Observers became curious about the causes of this expansion at an accelerating rate. Eventually, the cosmological constant "Λ" is held responsible for the aforementioned expansion. "Λ" represents the existence of dark energy. This constant "Λ" is a negative pressure fluid that provides the accelerating forces and opposes the NECs (null energy condition). Some amendments in GR (general relativity) were suggested to elaborate the late-time cosmic-accelerated behavior of the Universe by reducing the effects of DE (dark energy). GR is based on the symmetric and torsion-free Levi-Civita connection (Aldrovandi and Pereira, 2012) ($\Gamma^{\beta}_{\nu\mu} = \Gamma^{\beta}_{\mu\nu}$ and $T^{\lambda}_{\mu\nu} = 0$) and is well-known to deal with the local-level gravity. However, GR malfunctions in the discussion of gravity at a broader aspect, the global level. This malfunctioning of GR's global discussion of gravity generates the need for the modification of GR. Most of these modifications were based on the geometric extension of GR. $f(R)$ theories were pioneers among these modifications (Sotiriou and Faraoni, 2010; Bamba et al., 2012a). Here, R is the Ricci scalar used to express the Lagrangian function.

TEGR (teleparallel equivalent to general relativity) is a curvature-free torsion-based theory. A generalized version of TEGR is $f(T)$ gravity, which has close correspondence with the $f(R)$ theory. In the $f(T)$ theory, torsion T defines its gravitational field action rather than the Lagrangian function. This theory depends upon the Weitzenbock connection, so it is a curvature-less theory and has non-zero torsion (Aldrovandi and Pereira, 2012). Einstein defined torsion-based gravity depending on space–time (Einstein and Preuss, 1925). In setting up TEGR field equations, a tetrad plays a key role instead of the metric function. Different tetrads give rise to different field equations. Good tetrad and bad tetrad are two types of tetrads known as off-diagonal and diagonal tetrads, respectively. The application of a diagonal tetrad generates some solar system limitations in $f(T)$ gravity (Iorio and Saridakis, 2012a; Xie and Deng, 2013a). Hence, the choice of a correct (good) tetrad frees the function "f" from the imposition of the aforesaid constraints. The use of a diagonal (bad) tetrad produces a theory that is only well settled with the Birkhoff theorem, but the Schwarzschild metric is not the solution to that particular theory. However, an off-diagonal (good) tetrad does not impose any constraint on the value of "f" or "T." In this work, we use an off-diagonal tetrad.

Being TEGR and GR equivalent theories, every solution of TEGR is also the solution of GR. So, the problems which remain unaddressed in GR also carry with TEGR. One of the problems faced by researchers is of cosmological constant Λ, which serves as the negative pressure fluid $p_\Lambda = -\rho_\Lambda$. When exploring the present behavior of accelerating the Universe, GR can only deal with it by adding a scalar field as an extra term. The observed value of Λ drastically varies from the expected value, and researchers term that issue as a "fine-tuning problem." According to the collective view of researchers, this problem can only be dealt with by modifying GR, including an extra scalar field, or by altering the standard model of physics. Some theories suggest that GR modification can describe the late-time cosmic expansion behavior without the involvement of Λ. Regarding the early Universe, the rapid expansion in observations is called the inflationary era. This rapid expansion cannot be handled by the cosmological constant. This situation can be elaborated in the best way by including a scalar field. GR also does not provide any knowledge about the beginning and nature of inflation. Modified gravity (Nojiri and Odintsov, 2007; Sotiriou and Faraoni, 2010; Capozziello and De Laurentis, 2011) collectively explains the inflationary era called early-time expansion and the present DE era. The problem of coincidence suggests that matter's energy density and end DE of the present day are the same. Some theorists also think that it is not an issue but merely a coincidence. However, some GR modifications may address this issue (Nojiri and Odintsov, 2007). Famaey and McGaugh (2012) and Clifton et al. (2012) have pointed out many more issues which cannot be addressed in detail by GR. However, when one generalizes TEGR to the $f(T)$ gravity theory, this similarity is scattered as we consider Lagrangian as a function of the torsion scalar (Ferraro and Fiorini, 2008; Fiorini and Ferraro, 2009). Due to this reason, $f(T)$ gravity is chosen as a strong applicant to elaborate the acceleration aspect of Universe expansion by eliminating the existence of DE (Li et al., 2011; Cardone et al., 2012).

When we consider modeling stellar structures, we have to deal with field equations. Like GR, $f(T)$ gravity field equations have second-order derivatives, while $f(R)$ gravity equations contain fourth-order derivatives (Nojiri and Odintsov, 2007), where Palatini's version of $f(R)$ gravity consists of second-order equations. So, EFEs in $f(T)$ gravity, being of the second order, are easier to solve than the equations of $f(R)$ gravity. Contrary to GR, $f(T)$ gravity equations of motion are non-variant under the Lorentz transformation (Li et al., 2011), so they display an extra degree of freedom. Therefore, the $f(T)$ theory tremendously explains the whole scenario of cosmic acceleration on a wider scale of observations, like the clustering of galaxies (Camera et al., 2014). However, the solar system and pulsar observations show good agreement with the GR theory (Will, 2006). Iorio and Saridakis (2012a) and Xie and Deng (2013a) attract attention toward constraints in the solar system dealing with $f(T)$ gravity. However, in this paper, as mentioned previously, we choose an off-diagonal tetrad to eliminate constraints to construct structures of compact objects of anisotropic nature in $f(T, \mathcal{T})$ gravity formulation by taking into account $f(T, \mathcal{T}) = \alpha T^n(r) + \beta \mathcal{T}(r) + \phi$, where $\mathcal{T}$ is a trace of EMT. In Dent et al. (2011), BTZ black hole solutions are built in the $f(T)$ theory to elaborate the three-dimensional $f(T)$ model's effects. Afterward, a range of solutions for charged, isotropic, and anisotropic fluid showing the presence of compact objects has been formulated in $f(T)$ gravity (Boehmer et al., 2011; Zubair and Abbas, 2016). $f(T, \mathcal{T})$ gravity is very similar to $f(R, T)$ gravity, the only difference being that the $f(T, \mathcal{T})$ theory utilizes $\mathcal{T}$ in place of R in $f(R, T)$ gravity. Some considerable literature reports explain the context of $f(T, \mathcal{T})$ gravity (Salako et al., 2020; Zubair et al., 2021).

Compact stars are formed during the evolutionary stage of ordinary stars. At this stage, radiating pressure due to nuclear fission taking place inside the star does not resist the gravitational forces, and stars collapse under their own weight. This collapsing of the ordinary star is famously called stellar death, which results in the formation of a new star called a compact star. At this stage, all the reservoirs of helium are burnt up, which stops the fusion process, so the temperature inside the star decreases with the increase in internal pressure. Due to this increase in inner pressure, all matter of the star combine to a very high density. Compact stars have a very high density and smaller radii as compared to ordinary stars. High-density compact objects like a pulsar and many other spinning stars having strong magnetic fields are among the main discoveries of astrophysics. One belief about compact objects is that their matter composition is of subatomic particles like baryons, leptons, mesons, and strange quark matter. However, exact observational data about the composition of these high-density objects are not available. Therefore, the native problem in the construction of their configurations faced by astrophysicists is the determination of geometry used and interior surface matter distribution. Some valuable works are present in the literature on the study of compact stars (Mustafa et al., 2020; Mustafa et al., 2021; Maurya et al., 2022). In the background of other modified theories of gravity, interesting aspects related to astrophysical compact objects have been extensively explored (Mustafa et al., 2022a; Mustafa et al., 2022b; Mustafa et al., 2023).

Initial studies write that matter distribution on spherical symmetry is based on isotropic (perfect) fluid. Due to this isotropic condition, $(p_r = p_t)$ on EFEs is applied as tangential and radial components of pressure coincide with each other. However, Jeans (1922) predicted the unusual conditions, which are dominant inside the interior of stellar objects, due to which involvement of the anisotropic factor was suggested for a good understanding of the distribution of matter inside heavenly objects. Anisotropy $(\Delta = p_t - p_r)$ is simply a measurement of deviation from isotropy. In Herrera and Santos (1997) and Mak and Harko (2002), a huge amount of detailed material is available to study the effects of anisotropy in stellar structures under spherical symmetry. In a relativistic stellar system, anisotropy is due to the existence of a variety of fluids, like a superfluid, magnetic or external field, phase transition, rotational motion, and other fluids. This work is under a static and spherically symmetric system of stellar objects, so anisotropy may arise due to the existence of superfluid or the elastic nature of superfluid or anisotropic fluid (Sawyer, 1972; Sokolov, 1980; Herrera and Santos, 1997). Ruderman's (1972) prediction in his pioneer study of anisotropy in astrophysics is that it is an inherent property in high-density nuclear matter distribution. Bowers and Liang (1974) predicted that anisotropy is the result of strong interactions superconductivity and superfluidity inside heavily dense matter. It is of note that in a diverse situation when the radial component p_r is not equal to the tangential component p_t of pressure $(p_t \neq p_r)$, anisotropy rises. This form of pressure is called anisotropic pressure. When the spatial gradient of the scalar field is non-zero, then the physical system generates anisotropic pressure. Herrera and Santos (1997) first discussed the detailed effects of local-level anisotropy on the self-gravitating system. After that, the effects of local anisotropy were discussed by Ivanov (2002) and Maurya et al. (2016) on static bodies having spherical symmetry.

The schematic study of this paper is as follows: in the IInd section of this paper, we discuss the basics of $f(T, \mathcal{T})$ gravity. The IIIrd section consists of the generalized solutions of $f(T, \mathcal{T})$ gravity FEs. In the IVth section, we evaluate the unknown parameters by matching conditions. The Vth section discusses the physical analysis of the evaluated results. In the VIth section, we conclude of the discussion of the study on compact objects.

2 Basic concepts of $f(T, \mathcal{T})$ gravity and derivation of field equations

Since TEGR is a very close modification of GR gravity, factually, $f(T)$ gravity is far different from TEGR as it is based on the function of torsion T. So, the description of $f(T)$ gravity is considerably different from the curvature-dependent $f(R)$ gravity. In particular, the action elaborates on the Lagrangian function of gravity. The action (Harko et al., 2014) describing $f(T, \mathcal{T})$ is given as follows:

$$s = \int dx^4 e \left\{ \frac{1}{2k^2} f(T, \mathcal{T}) + \mathcal{L}_{(M)} \right\}, \tag{1}$$

where $\mathcal{L}_{(M)}$ expresses the Lagrangian density and f is the function based on torsion T and trace $\mathcal{T}$. Here, $e = det\left(e_\mu^A\right) = \sqrt{-g}$ and $k^2 = 8\pi G = 1$. The generalized version of EFE is derived from

Eq. 1 expressing the Lagrangian, which is presented as follows (Harko et al., 2014):

$$\begin{aligned}
&e_i{}^\gamma S_\gamma{}^{\mu\eta} f_{TT} \partial_\mu T + e_i{}^\gamma S_\gamma{}^{\mu\eta} f_{T\mathcal{T}} \partial_\mu \mathcal{T} + e^{-1} \partial_\mu \left(e e_i{}^\gamma S_\gamma{}^{\mu\eta} \right) f_T - e_\eta{}^i T^\gamma{}_{\mu i} S_\gamma{}^{\eta\mu} f_T \\
&- \frac{1}{4} e_i{}^\eta f + f_\mathcal{T} \omega^\gamma{}_{\eta\mu} S_\gamma{}^{\eta\mu} - \frac{f_\mathcal{T}}{2} \left(e_\eta{}^i T_i{}^\eta + p_t e_\eta{}^i \right) = -4\pi e_\eta{}^i T_i{}^\eta. \tag{2}
\end{aligned}$$

Here, T_i^ν is the energy–momentum tensor, and derivatives of function f are $f_T = \frac{\partial f}{\partial T}$, $f_{TT} = \frac{\partial^2 f}{\partial T^2}$, $f_\mathcal{T} = \frac{\partial f}{\partial \mathcal{T}}$, and $f_{T\mathcal{T}} = \frac{\partial^2 f}{\partial T \partial \mathcal{T}}$. Other basic concepts used in Eq. 2 like torsion contorsion and super-potential are defined as follows (Harko et al., 2014):

$$T^\lambda{}_{\mu\eta} = e_\vartheta{}^\lambda \left(\partial_\mu e^\vartheta{}_\eta - \partial_\eta e^\vartheta{}_\mu \right) + \omega^\gamma{}_{\eta\mu}, \tag{3}$$

$$K_\lambda{}^{\mu\eta} = -\frac{1}{2} \left(T^{\mu\eta}{}_\lambda - T^{\eta\mu}{}_\rho - T_\lambda{}^{\mu\eta} \right), \tag{4}$$

$$S_\lambda{}^{\mu\eta} = \frac{1}{2} \left(K^{\mu\eta}{}_\lambda + \delta^\mu{}_\lambda T^{\gamma\mu}{}_\gamma - \delta^\eta{}_\lambda T^{\gamma\mu}{}_\gamma \right). \tag{5}$$

Like TEGR, the Lagrangian density, depending upon the torsion T, is written, in general, as follows (Harko et al., 2014):

$$T = T^\lambda{}_{\kappa\eta} S_\lambda{}^{\kappa\eta}. \tag{6}$$

Since spherical symmetry is a convenient way to start with the study of compact objects, which is written as

$$ds^2 = e^{\nu(r)} dt^2 - e^{\lambda(r)} dr^2 - r^2 d\theta^2 - r^2 \sin^2\theta d\phi^2, \tag{7}$$

where $\nu(r)$ and $\lambda(r)$ the gauge ingredients describing the gravity are the radial r functions.

Importantly, in TEGR, the prescription of the tetrad field harmonizes both the gravitational field and the reference frame. In the calculation of field equations, the tetrad field plays a defining role. Tamanini and Boehmer (2012) nominated two types of tetrads: off-diagonal and diagonal. They suggested that the use of a diagonal tetrad imposes few solar system limitations, as expressed in Iorio and Saridakis (2012a) and Xie and Deng (2013a). Here, in the current study, we incorporate an off-diagonal tetrad to reduce the impact of limitations that were discussed in Iorio and Saridakis (2012a) and Xie and Deng (2013a). The off-diagonal tetrad is given as follows:

$$e_\gamma^\eta = \begin{pmatrix} e^{\frac{\nu(r)}{2}} & 0 & 0 & 0 \\ 0 & e^{\frac{\lambda(r)}{2}} \sin\theta\cos\phi & r\cos\theta\cos\phi & -r\sin\theta\sin\phi \\ 0 & e^{\frac{\lambda(r)}{2}} \sin\theta\sin\phi & r\cos\theta\sin\phi & r\sin\theta\cos\phi \\ 0 & e^{\frac{\lambda(r)}{2}} \cos\theta & -r\sin\theta & 0 \end{pmatrix}, \tag{8}$$

where the notation e is used for e_γ^η, which is equal to $e^{\nu(r)+\lambda(r)} r^2 \sin\theta$. In this current study, we utilize the off-diagonal tetrad by taking $\omega^\gamma{}_{\eta\mu} = 0$. Fluid distribution of an anisotropic nature is defined as

$$T_{\nu\mu}^{(m)} = \left(\rho + p_t \right) u_\nu u_\mu - p_t g_{\nu\mu} + \left(p_r - p_t \right) v_\nu v_\mu, \tag{9}$$

where $u_\nu = e^{\frac{\mu}{2}} \delta_\nu^0$ and $v_\nu = e^{\frac{\nu}{2}} \delta_\nu^1$, and ρ, p_r, and p_t represent the function forms of the energy density and radial and tangential pressures, respectively. Here, $T_{\nu\mu}^{(m)} = [\rho, -p_r, -p_t, -p_t]$. The trace term of the energy–momentum tensor is expressed as

$$\mathcal{T} = \delta_\mu^\nu T_\nu^\mu. \tag{10}$$

The expression of torsion $T(r)$ calculated from equation (6) and its derivative $T'(r)$ relative to "r" are written as

$$T(r) = \frac{2e^{-\lambda(r)}\left(e^{\frac{\lambda(r)}{2}}-1\right)\left(e^{\frac{\lambda(r)}{2}}-rv'(r)-1\right)}{r^2}, \qquad (11)$$

$$T' = -\frac{4e^{-\lambda(r)}\left(e^{\frac{\lambda(r)}{2}}-1\right)\left(e^{\frac{\lambda(r)}{2}}-rv'(r)-1\right)}{r^3} + \frac{e^{-\frac{\lambda(r)}{2}}\lambda'(r)\left(e^{\frac{\lambda(r)}{2}}-rv'(r)-1\right)}{r^2}$$
$$-\frac{2e^{-\lambda(r)}\left(e^{\frac{\lambda(r)}{2}}-1\right)\lambda'(r)\left(e^{\frac{\lambda(r)}{2}}-rv'(r)-1\right)}{r^2}$$
$$+\frac{1}{r^2}2e^{-\lambda(r)}\left(e^{\frac{\lambda(r)}{2}}-1\right)\left[\frac{1}{2}e^{\frac{\lambda(r)}{2}}\lambda'(r)-rv''(r)-v'(r)\right]. \qquad (12)$$

The generalized field expressions of ρ, p_r, and p_t in $f(T,\mathcal{T})$ gravity are obtained by using Eqs 2, 7, 8.

$$\rho = -\frac{e^{-\frac{\lambda(r)}{2}}\left(e^{-\frac{\lambda(r)}{2}}-1\right)(f_{TT}T'+f_{T\mathcal{T}}\mathcal{T}')}{r}$$
$$-\frac{1}{2}f_T\left(-\frac{e^{-\lambda(r)}(1-r\lambda'(r))}{r^2}-\frac{1}{r^2}+\frac{T(r)}{2}\right)+\frac{f}{4}+\frac{1}{2}f_\mathcal{T}\times(p_t+\rho), \quad (13)$$

$$p_r = \left(\frac{e^{-\lambda(r)}(rv'(r)+1)}{r^2}-\frac{1}{r^2}+\frac{T(r)}{2}\right)\frac{f_T}{2}-\frac{f}{4}-\frac{1}{2}f_\mathcal{T}(p_t-p_r), \qquad (14)$$

$$p_t = \frac{1}{2}e^{-\lambda(r)}\left(-\frac{e^{\frac{\lambda(r)}{2}}}{r}+\frac{v'(r)}{2}+\frac{1}{r}\right)(f_{TT}T'+f_{T\mathcal{T}}\mathcal{T}')$$
$$+\left[e^{-\lambda(r)}\left(\left(\frac{v'(r)}{4}+\frac{1}{2r}\right)(v'(r)-\lambda'(r))+\frac{v''(r)}{2}\right)+\frac{T(r)}{2}\right]\frac{f_T}{2}-\frac{f}{4}, \qquad (15)$$

where T represents the torsion and $\mathcal{T}$ represents the trace of the energy–momentum tensor.

3 Generalized solutions

Solutions of the field equations mainly depend upon the functions of gravitation-responsible components of the metric space. We take the function $\lambda(r)$ given by Solanki and Jackson Levi Said (2022)

$$\lambda(r) = \left(\frac{cr^2}{R^2}+1\right)^2. \qquad (16)$$

Here, c,R are constants with $c,R > 0$, and R is the radius at the boundary of the star. The potential metric (16) is a valid physical concept since it remains non-singular when $c > 0$ within the interior of a star, where $0 \le r \le R$. This metric potential (16) is highly beneficial for describing various astrophysical phenomena. It has been used in simplified forms, such as in (16), to describe compact stars under general relativity (Sarma and Ratanpal, 2013). Conversely, its inverse has been utilized to depict wormholes in f (T) gravity (Jamil et al., 2013). Hence, the parameter c plays a crucial role in characterizing neutron stars that exhibit realistic masses. As discussed in the section, it is evident that the model parameter c holds significant physical importance, given its considerable

influence on modeling stellar systems. Now, we select another metric potential $e^{v(r)}$ such that $v'(r)$ has the following form (Solanki and Jackson Levi Said, 2022):

$$v'(r) = \frac{\frac{r^5 z}{R^6}+\frac{r^3 y}{R^4}+\frac{rx}{R^2}}{\frac{cr^2}{R^2}+1}, \qquad (17)$$

where x, y, z, and R are constant parameters, where R represents the radius of a star and r is the radial coordinate. It is important to note that the constants x, y, and z have no relation to the space coordinates. Rather, they represent the model parameters and should not be confused with spatial coordinates. Integration of Eq. 17 results in the following form:

$$e^{v(r)} = ke^{\left(\frac{r^2(cy-z)}{2c^2R^2}+\frac{r^4 z}{4cR^4}\right)}\left(\frac{cr^2}{R^2}+1\right)^{\frac{c^2x-cy+z}{2c^3}}. \qquad (18)$$

The function f defines the modified form of $f(T,\mathcal{T})$. In this study, we take the most generic modification of $f(T,\mathcal{T})$ gravity, which is very similar to the model suggested by Harko et al. (2014):

$$f(T,\mathcal{T}) = \alpha T^n(r) + \beta\mathcal{T}(r) + \phi, \qquad (19)$$

where $\alpha\,\beta$ are arbitrary constants and ϕ is a cosmological constant. If we set $n = 2$ and $\phi = 0$, this model reduces to the model used by Harko et al. (2014). This model 19 can be reduced to some generic torsion-based theories like $f(T)$ gravity and TEGER depending upon the choice of parameters α, β and n. Taking $\beta = 0$ for different choices of n, we retrieve the $f(T)$ gravity, and by choosing $\alpha = 1, n = 1, \phi = 0, \text{and}\beta = 0$, we retrieve the basic TEGER. In this study, we use the value $n = 2$ by taking the non-linear model of $f(T,\mathcal{T})$ gravity. Results are also good and acceptable for $n = 1$ (Zubair et al., 2021), but for other integral values of n, results do not lie within the admissible range. Moreover, by incorporating the trace term $\mathcal{T} = \rho - p_r - 2p_t$, it is possible to investigate the minimal coupling between torsion and matter contributions. Prior studies have focused on compact star models within the context of $f(R,T) = R + \lambda T$, which exhibits minimal coupling between curvature and torsion components (Zubair et al., 2016; Maurya et al., 2019; Rahaman et al., 2020; Waheed et al., 2020). Such investigations are critical for exploring compact star models within a minimally coupled torsion-based framework and for generating new interpretations of possible outcomes. In this study, ϕ denotes the cosmological constant (Behar and Carmeli, 2000), which defines the various phases of Universe expansion. A universe with a positive ϕ accelerates, whereas a negative ϕ results in deceleration, stopping, and reversing of the expansion (Carmeli and Kuzmenko, 2001). According to calculations, the value of the cosmological constant must be $\phi = 2.036 \times 10^{-35}s^{-2}$ (Carmeli and Kuzmenko, 2001). Furthermore, in their work on the linear model $f(T,T) = \alpha T(r) + \beta T(r) + \phi$, Pace and Said (2017) employed the same positive value of ϕ to investigate quark stars within $f(T,T)$ gravity. In this study, we also use the positive calculated value of ϕ to examine the accelerated phase of Universe expansion. By using Eqs 11–15, 19 and putting the metric components from Eqs 16, 18, we obtain the simplified expressions of $\rho, p_r, \text{and}p_t$ as follows:

$$\rho = -\frac{4\left(1-\frac{3\beta}{4}\right)}{8\left(-\beta^2+3\beta-2\right)r^4}$$
$$\times\Bigg[\Bigg[-\frac{\alpha l_5(r)\,2^{n+2}(n-1)\,nr^4R^4}{(l_1(r)-1)\left(-cr^2R^4(l_1(r)-1)-R^6(l_1(r)-1)+r^6z+r^4R^2y+r^2R^4x\right)^2}$$
$$\times\left[c^4r^8+4c^3r^6R^2-c^2r^4R^4(4l_1(r)-9)+cr^2\left[-r^4R^2y(l_1(r)-2)-r^2R^4x(2l_1(r)-3)\right.\right.$$
$$\left.-2R^6(3l_1(r)-4)+r^6z\right]-R^2(l_1(r)-1)\left(-2r^2z-r^4R^2y+2R^6\right)\right]+\frac{\alpha l_3(r)\,2^n nr^2}{l_2^2(r)R^4(cr^2+R^2)}$$
$$\left[2l_2(r)R^4(cr^2+R^2)-4cr^2R^4+r(l_1(r)-1)(r^5z+r^3R^2y+rR^4x)\right]+\alpha l_4(r)\,2^n r^4+r^4\phi\right]$$
$$+\beta r^2\left[\frac{\alpha l_3(r)\,2^n n}{l_2^2(r)}\left(\frac{r^2(l_1(r)-2)(r^4z+r^2R^2y+R^4x)}{cr^2R^4+R^6}+2(l_2(r)-1)\right)\right.$$
$$\left.+\alpha l_4(r)\,2^n r^2+r^2\phi\right]\Bigg]\Bigg], \tag{20}$$

$$p_r = \frac{(l_2(r)-1)}{8\left(\beta^2-3\beta+2\right)(l_2(r)-1)\left(\frac{r^6z+r^4R^2y+r^2R^4x}{cr^2R^4+R^6}-l_2(r)+1\right)^2}$$
$$\times\Bigg[\Bigg[2\left[\frac{\alpha\beta l_5(r)\,2^n(n-1)nr^2}{R^4(cr^2+R^2)^2}\left(c(3r^6z+r^4R^2y-r^2R^4x)+5r^4R^2z\right.\right.$$
$$\left.+3r^2R^4y+R^6x\right)+\alpha l_4(r)\,2^n\left[(\beta-2)l_2^2(r)+2l_2(r)(n-1)\,(\beta+\beta n-2)\right.$$
$$\left.\left.-(2n-1)(\beta+\beta n-2)\right]+(\beta-2)\phi(l_2(r)-1)^2\right]-\frac{\alpha\beta cl_5(r)\,2^{n+2}n(2n-3)r^2}{cr^2+R^2}\right]$$
$$\times\frac{r(r^5z+r^3R^2y+rR^4x)}{R^6\left(\frac{cr^2}{R^2}+1\right)}\left[-\frac{\alpha\beta cl_4(r)\,2^{n+2}nr^2(l_2(r)(n-1)-2n+3)}{R^2\left(\frac{cr^2}{R^2}+1\right)}+\alpha l_4(r)\,2^n\left[-4\beta+2(\beta-2)\right.\right.$$
$$\times l_2^2(r)(n-2)+l_2(r)\left(8(\beta-2)-2\beta n^2+(20-9\beta)n\right)+2\beta n^2+(9\beta-16)n+8\right]-4(\beta-2)\phi(l_2(r)-1)^2\Bigg]$$
$$+\frac{(r^6z+r^4R^2y+r^2R^4x)^2\left(2(\beta-2)\phi(l_2(r)-1)-\alpha l_4(r)\,2^n(2\beta+2(\beta-2)l_2(r)(n-1)-5\beta n+8n-4)\right)}{l_2^2(r)R^{12}}\Bigg], \tag{21}$$

$$p_t = \frac{1}{8(l_2(r)-1)^2\left(-l_2(r)+\frac{zr^6+R^2yr^4+R^4xr^2}{R^6+cr^2R^4}+1\right)^2(\beta-2)(\beta-1)}$$
$$\times\Bigg[\frac{2^nl_5(r)\,nr^6(l_1(r)-1)}{R^{12}(cr^2+R^2)^3}(zr^4+R^2yr^2+R^4x)^3\alpha(\beta-1)-\frac{(l_2(r)-1)(zr^5+R^2yr^3+R^4xr)}{\left(\frac{cr^2}{R^2}+1\right)R^6}$$
$$\times\left[-2^{n+3}l_4(r)\,\alpha l_2^2(r)+2^{n+3}l_4(r)\,nl_2^2(r)\,\alpha-3\cdot2^{n+1}nl_4(r)\,\alpha\beta l_2^2(r)+2^{n+2}l_4(r)\,\alpha\beta l_2^2(r)\right.$$
$$-8\phi l_2^2(r)+4\beta\phi l_2^2(r)-2^{n+3}n^2l_4(r)\,\alpha-2^{n+1}l_4(r)\,\alpha-13\cdot2^{n+1}nl_2(r)\,l_4(r)\,\alpha$$
$$9\cdot2^{n+1}l_4(r)\,n\alpha+-2^{n+3}l_2(r)\,l_4(r)\,n^2\alpha+2^{n+4}l_2(r)\,l_4(r)\,\alpha+3\cdot2^{n+1}l_4(r)\,n^2\alpha\beta$$
$$+2^{n+2}l_4(r)\,\alpha\beta-11\cdot2^nnl_4(r)\,\alpha\beta 2^{n+3}l_2(r)\,l_4(r)\,\alpha\beta-3\cdot2^{n+1}n^2l_2(r)\,l_4(r)\,\alpha\beta$$
$$+15\cdot2^nl_2(r)\,l_4(r)\,n\alpha\beta+16l_2(r)\,\phi-8l_2(r)\,\beta\phi+4\beta\phi-8\phi$$
$$-\frac{2^{n+2}cnr^2l_4(r)\,\alpha(-4\beta n+6n+l_2(r)(n(\beta-2)+1)-3)}{\left(\frac{cr^2}{R^2}+1\right)R^2}-\frac{2^{n+1}n^2r^2l_5(r)}{R^4(cr^2+R^2)^2}$$
$$\times\left[xR^6+3r^2yR^4+5r^4zR^2+c(3zr^6+R^2yr^4-r^2R^4x)\right]\alpha(\beta-1)\right]r+$$
$$\times\frac{(zr^6+R^2yr^4+R^4xr^2)^2}{l_2^2(r)R^{12}}\left[(l_2(r)-1)\left[2(l_2(r)-1)(\beta-2)\phi-2^nl_4(r)\,\alpha(2(\beta-1)n^2+{}+(9-6\beta)n\right.\right.$$
$$\left.+2(\beta-2)+l_2(r)(-2\beta+n(3\beta-5)+4))\right]-\frac{2^{n+2}cnr^2(n(l_1(r)-2)+1)l_5(r)\,\alpha(\beta-1)}{cr^2+R^2}\right]$$
$$+(l_2(r)-1)^2\left[\frac{2^{n+2}cl_5(r)\,nr^2\alpha(2n(\beta-2)+\beta+2)}{cr^2+R^2}\right]$$
$$+2\left[-\frac{2^nnl_5(r)(xR^6+3r^2yR^4+5r^4zR^2+c(3zr^6+R^2yr^4-r^2R^4x))\alpha(n(\beta-2)+1)r^2}{R^4(cr^2+R^2)^2}\right.$$
$$-2^nl_4(r)\,\alpha(r(2n(\beta-1)-\beta+2)l_2^2(r)-(2n^2-3n+1)(\beta-2)+2l_2(r)(n-1)^2(\beta-2))$$
$$\left.+(l_2(r)-1)^2(\beta-2)\phi\Bigg]\Bigg]. \tag{22}$$

4 Matching of the interior metric with the exterior metric to evaluate unknowns

At the boundary surface, $r=R$ and the matching of the interior and exterior metrics is essential to make the unknowns known. In this study, we match the interior space–time (Eq. 7) with the exterior Schwarzschild space–time (Eq. 23) to evaluate k. We evaluate α from $p_r(r=R)=0$. The exterior Schwarzschild metric is given as

$$ds^2=\left(1-\frac{2M}{R}\right)dt^2-\left(1-\frac{2M}{R}\right)^{-1}dr^2-r^2\left(d\theta^2+\sin^2\theta d\phi^2\right). \tag{23}$$

Matching Eqs 7, 23 we obtain the following system of equations.

$$\left(\frac{cr^2}{R^2}+1\right)^2=\left(1-\frac{2M}{R}\right)^{-1}, \tag{24}$$

$$ke^{\left(\frac{r^2(cy-z)}{2c^2R^2}+\frac{r^4z}{4cR^4}\right)}\left(\frac{cr^2}{R^2}+1\right)^{\frac{c^2x-cy+z}{2c^3}}=1-\frac{2M}{R}, \tag{25}$$

$$p_r(r=R)=0. \tag{26}$$

The solution of the aforementioned Eqs. 25, 26 gives the value of $k\$,\$$ and Eq. 26 gives the value of α having the following expression forms:

$$k=e^{-\frac{2cy+cz-2z}{4c^2}}(c+1)^{-\frac{4c^3+c^2x-cy+z}{2c^3}}, \tag{27}$$

$$\alpha=\frac{(\beta-2)(L-1)\,2^{1-n}\phi(c(-L)+c-L+x+y+z+1)^2\left(\frac{(L-1)(c(L-1)+L-x-y-z-1)}{(c+1)^3R^2}\right)^{-n}}{N}, \tag{28}$$

where

$$L=\sqrt{(1+c)^2},$$
$$N=2c^4\left((\beta-2)(L-3)+2\beta n^2-4n\right)+2c^3\left[2(\beta-2)(2L-x-y-z-6)\right.$$
$$+8\beta n^2+n((\beta-2)x+(\beta-2)y+\beta z-2z-16)\right]-2c^2\left[2\beta(4L-9)n^2\right.$$
$$-n(-5\beta+5\beta L+8L+3(\beta-2)x+3(\beta-2)y+3\beta z-6z-28-(\beta-2)]$$
$$+(9L-6x-6y-6z-19)]-c\left[4\beta n^2((2L-3)x+(L-2)y+6L-z-8)\right.$$
$$+n(8\beta-8\beta L+x(\beta(3L-1)-20L+28)+y(-5\beta+7\beta L-20L+28)$$
$$+11\beta Lz-20Lz-32L-9\beta z+28z+48)-4(\beta-2)(2(L-2)x+2(L-2)y$$
$$+2Lz+5L-4z-7)]+4\beta(L-1)n^2\times(y+2z-2)-n[-2\beta+2\beta L+x^2$$
$$\times(\beta(2L-5)-4L+8)+x(-13\beta+11\beta L+2y(\beta(2L-5)-4L+8))$$
$$+2z(-5\beta+2\beta L-4L+8)-20L+20)+y^2(\beta(2L-5)-4L+8)+y$$
$$\times(\beta(15L-17)+2z[\beta(2L-5)-4L+8]-20L+20)+2\beta Lz^2-4Lz^2$$
$$+19\beta Lz-20Lz-16L-5\beta z^2+8z^2-21\beta z+20z+16+2(\beta-2)$$
$$\times(L-1)(x+y+z+2)^2.$$

For other constants, i.e., c,x,y,z,ϕ,β, we choose suitable values, as given in Table 1.

5 Physical analysis and discussion of the calculated results

In this section, we analyze the results of our study by discussing the physical behavior of some properties of neutron stars (4U1538−52, J0437−4715, J0030 + 0451, and 4U1820−30) under the parameters of $f(T,\mathcal{T})$ gravity by coupling the trace term with the torsion and using the off-diagonal tetrad.

5.1 Metric potentials and energy density

As the responsibility of gravitational effects is mainly dependent upon the metric function, for the study of compact objects, these metric functions must be positive and smooth. As can be easily verified from their graphical results (graphed in the left panel of

TABLE 1 Values of constants of strange stars for $n = 2$, $y = -0.04$, $z = -0.0009$, $\phi = 2.036 \times 10^{-35}$, and $\beta = -30$ by choosing different values of c and β in the case of the off-diagonal tetrad.

Name of the star	Observed mass	Predicted radius	c	x	k	α
4U1538−52	0.827	10.060	0.32	0.9	0.391689	-1.22734×10^{-30}
J0437−4715	1.440	13.972	0.28	0.8	0.432662	-4.01855×10^{-30}
J0030 + 0451	1.5	12.350	0.29	0.95	0.399381	-1.55632×10^{-30}
4U1820−30	1.460	10.602	0.42	1.35	0.284537	-1.34009×10^{-30}

FIGURE 1
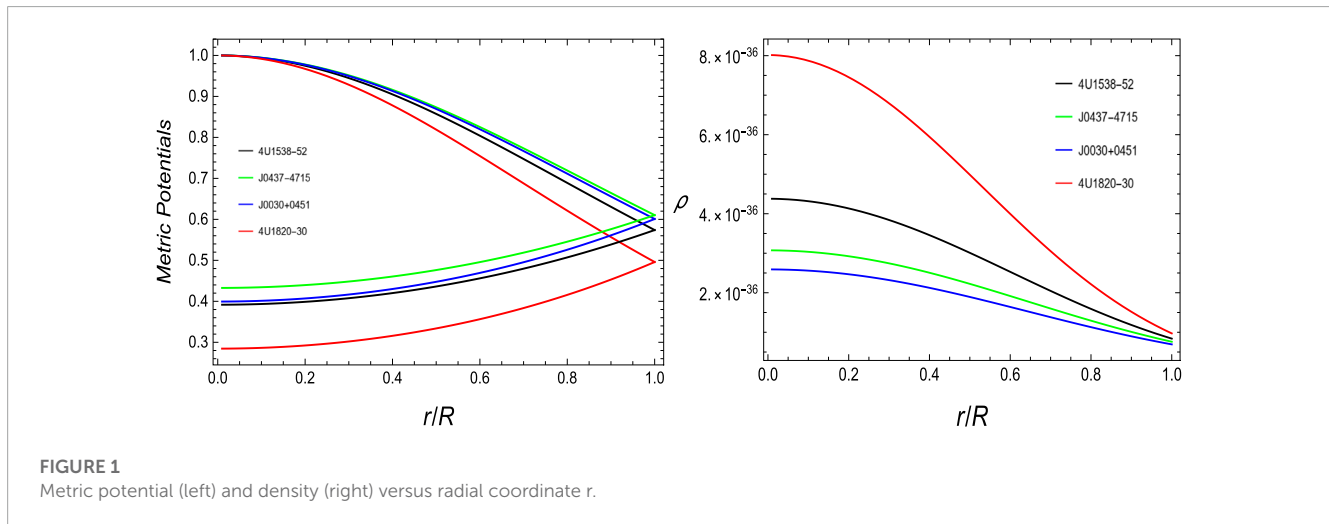Metric potential (left) and density (right) versus radial coordinate r.

Figure 1), $e^{\lambda(r)} = 1$ (at the center) and $e^{\nu(r)} > 0$ (at the center) show positive and regular monotonic responses throughout the interior of the stellar system.

The importance of verifying the physical validity of stellar configurations in compact star research cannot be overstated. Any study lacking physical acceptability would render any effort invested in it meaningless. Density serves as a crucial parameter for ensuring the validity of such studies. The validity of the distribution of matter can be determined from the behavior of the energy density ρ, as shown graphically. For the physical presence of a compact star, the energy must be positive, maximal at the center, and have a decreasing trend with a minimal value at the boundary. The right graph in Figure 1 depicts the visualization of the behavior of energy density for our neutron star candidates, which falls completely within the required criteria.
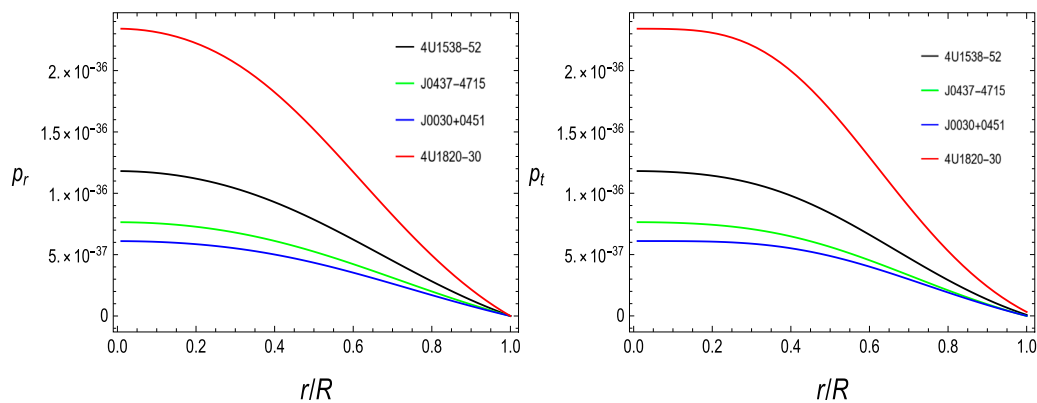
5.2 Pressure profiles

It is important to consider pressure components as another crucial parameter when assessing the validity of a stellar model. By following a similar trend as the density profile, the realistic distribution of stellar pressure profiles should also contain the positive and maximum values at the center and then decreasing propagation throughout the stellar system with a minimum value at the boundary; in addition, $p_r|_{r=R} = 0$; otherwise, $p_t \,\&\, p_r$ remain positive and $p_t > p_r$. Figure 2 shows the graphical representation of the pressure profiles. It should be noted that the behavior of pressure

profiles is a genuine indicator of the physical existence of a stellar system in our case.
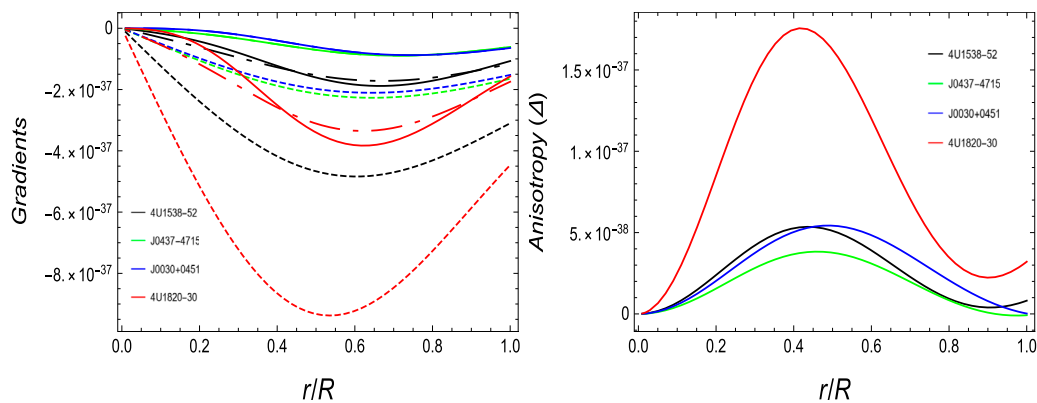
5.3 Gradients and anisotropy profiles

The graph of gradients is plotted in the right of Figure 3. It is required that for the compact formation of stellar configuration, the gradients should attain the negatively increasing trend starting from zero at the center to the boundary of the stellar configuration. In our study, it can easily be seen that $\frac{d\rho}{dr}|_{(0<r\leq R)} \leq 0$, $\frac{dp_r}{dr}|_{(0<r\leq R)} \leq 0$, $\frac{dp_t}{dr}|_{(0<r\leq R)} \leq 0$. Our analysis led us to the conclusion that all the derivatives of matter density, radial pressure, and tangential pressure are negative and display a decreasing trend. The negative values of these gradients indicate that the solutions we have obtained are physically feasible and satisfy a fundamental requirement for celestial modeling.

Anisotropy is another important property of the stellar system that justifies the stability system. The existence of positive anisotropy ($\Delta > 0$) is basically a repulsive force against the inward gravitational force and keeps the system stable. Basically, the distribution of matter all over the stellar may not be uniform, which may cause the existence of anisotropy. The pressure profiles at the center of the star are identical, due to which $\Delta \mid_{r=0} = p_t - p_r = 0$, but it attains the peak value at the boundary $r = R$. The graphical conduct of the anisotropic profile is given in the right graph of Figure 3. It can easily be verified that it starts its propagation from zero at the center and attains the maximum value, and afterward, it again starts to decline

FIGURE 2
Radial and tangential pressures versus the radial coordinate r.

FIGURE 3
Gradients (left) and anisotropy (right) versus the radial coordinate r.

and approaches zero for some candidates of neutron stars and subsequently shows an uplift in the value at the boundary. However, the overall trend is positive ($\Delta > 0$) within the stellar system to justify the stability.

5.4 Energy conditions

The real essence of the matter in the stellar system is studied by energy constraints. The positive behavior of energy constraints in the complete spread of the stellar body justifies and ensures the real and physically acceptable distribution of matter of anisotropic form. Energy limits named SEC, WEC, NEC, and DEC should justify the given following conditions (29–32) during propagation in the compact formation of stellar bodies.

$$SEC: \rho + p_\gamma \geq 0, \quad \rho + p_r + 2p_t \geq 0, \tag{29}$$

$$WEC: \rho \geq 0, \quad \rho + p_\gamma \geq 0, \tag{30}$$

$$NEC: \rho + p_\gamma \geq 0, \tag{31}$$

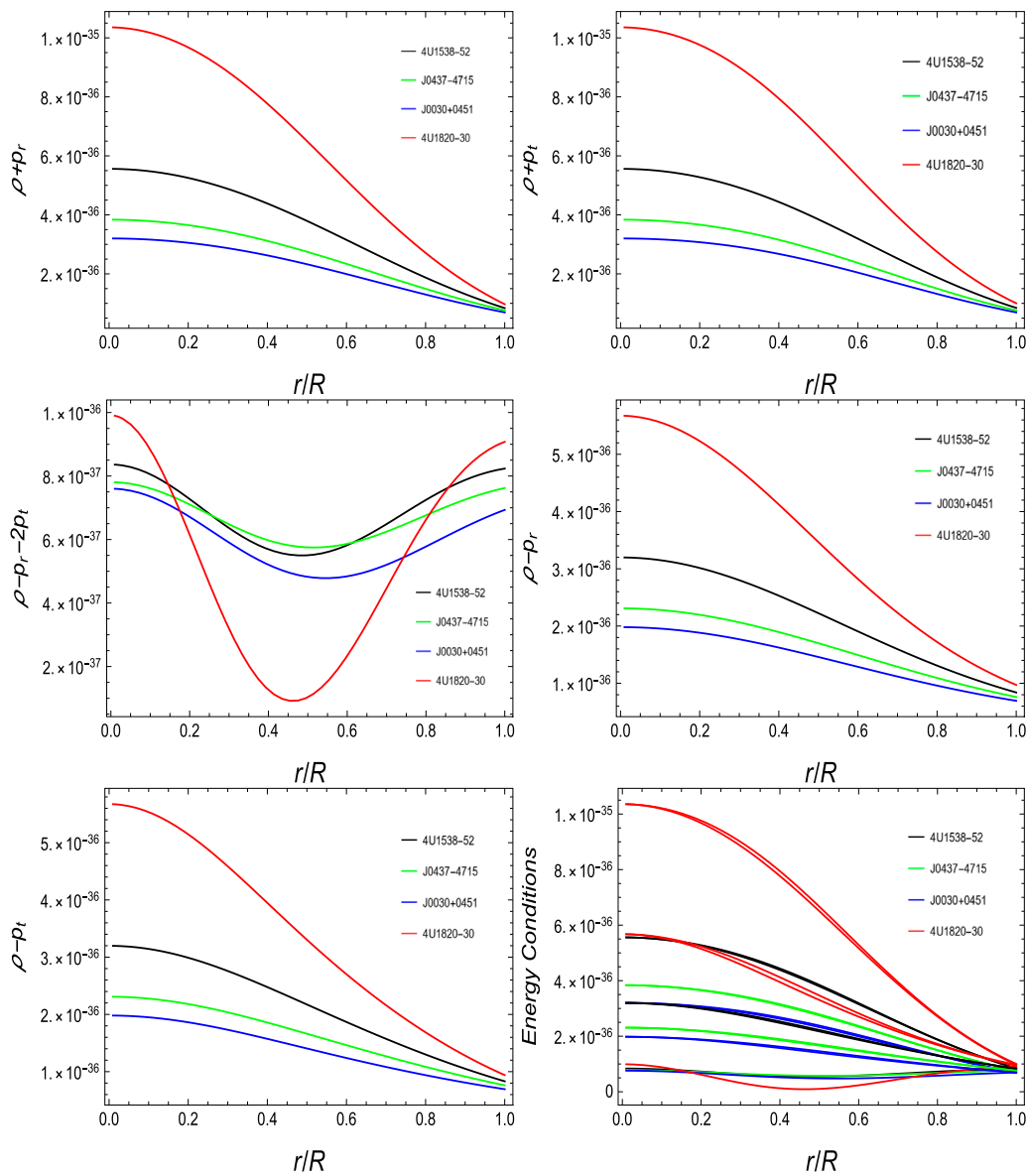$$DEC: \rho > |p_\gamma|, \tag{32}$$

where $\gamma = r, t$. The graphical representation of energy conditions in Figure 4 indicates the real formation of compact matter in our neutron star candidates in the gravitational effects of $f(T, \mathcal{T})$ gravity.

5.5 Sound speeds

Sound speeds v_r^2 & v_t^2 are two other important aspects to study the stability of the compact stellar system. The cracking concept introduced by Herrera for the anisotropic nature of matter is an addition to the stability discussion of the stellar system. This cracking concept (Herrera, 1992) defines the stability by two constraints $0 < v_r^2$ & $v_t^2 < 1$, where $c = 1$ is the speed of light, which means both the sound speeds must be less than c, the speed of light. Expressions for sound speeds are as follows:

$$v_r^2 = \frac{dp_r}{d\rho} \quad \& \quad v_t^2 = \frac{dp_t}{d\rho}. \tag{33}$$

According to the stability region defined in Abreu et al. (2007), the region is stable, in which $v_r^2 > v_t^2$, and there is no change of sign in

FIGURE 4
Energy conditions versus the radial coordinate.

$v_r^2 - v_t^2$. After that, Andreasson (2008) generalized this criterion limit as $0 < |v_t^2 - v_r^2| < 1$ by introducing the concept of no cracking where the region is stable. Figure 5 and the right of Figure 6 justify that all the stability limits are justified in our study of neutron stars.

5.6 TOV forces

Stability and equilibrium of the stellar system are also discussed and recommended with the help of well-famed criteria suggested in the Tolman–Oppenheimer–Volkoff (TOV) equation (Oppenheimer and Volkoff, 1939; Tolman, 1939). The TOV equation in its most common version of GR is defined as

$$\frac{dp_r}{dr} + \frac{M_g(r)(\rho + p_r)}{r} e^{\frac{v-\lambda}{2}} - \frac{2(p_t - p_r)}{r} = 0, \tag{34}$$

where $M_g(r)$ is the gravitational mass present inside the radius of stellar radius r and can be evaluated by using the Tolman–Whittaker formula and FEs, which is given by

$$M_g(r) = 4\pi \int_0^r \left(T_t^t - T_r^r - T_\theta^\theta - T_\phi^\phi \right) r^2 e^{\frac{v+\lambda}{2}} \, dr. \tag{35}$$

Eq. 35 can mold its form given by the following expression:

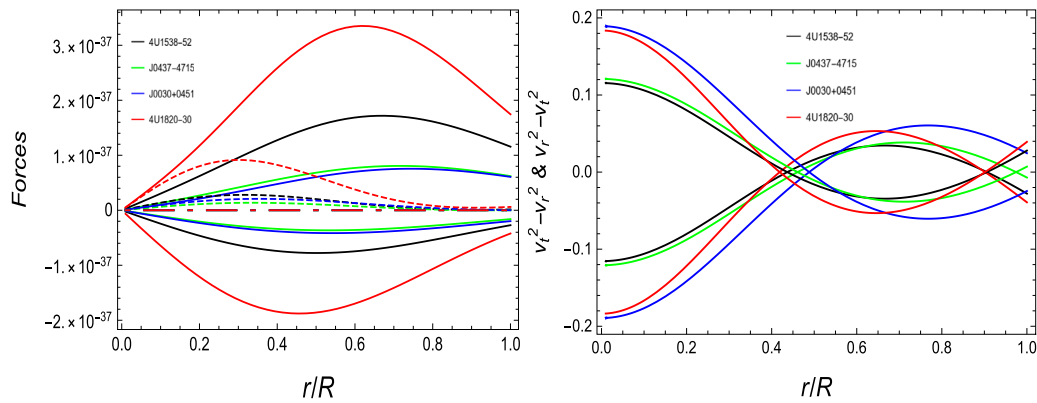$$M_g(r) = \frac{2}{2} r e^{\frac{\lambda-v}{2}} v'. \tag{36}$$

By substituting the value of $M_g(r)$ from Eq. 36 into Eq. 34, we obtain

$$\frac{dp_r}{dr} + \frac{v'(\rho + p_r)}{r} - \frac{2(p_t - p_r)}{r} = 0. \tag{37}$$

Equation 37 is the generic GR version of the TOV equation, but in the case of $f(T, \mathcal{T})$ gravity, an extra term is available, so Eq. 37, in the

FIGURE 5
Sound speeds v_{sr}^2 (left) and v_{st}^2 (right) versus the radial coordinate r.

FIGURE 6
Forces (left) F_h(solid−positive), F_g(solid−negative), F_a(dotted), F_e(dot-dashed) and casuality conditions (right) versus the radial coordinate.

case of $f(T, \mathcal{T})$ gravity, takes the following form:

$$\frac{dp_r}{dr} + \frac{v'(\rho + p_r)}{2} - \frac{2(p_t - p_r)}{r} - \frac{-\frac{1}{4}\beta\frac{dp_r}{dr} - \beta\frac{dp_t}{dr} + \frac{1}{4}\beta\frac{d\rho}{dr}}{\frac{\beta}{2} + 4\pi} = 0, \quad (38)$$

$$F_g + F_h + F_a + F_e = 0, \quad (39)$$

where

$$F_g = -\frac{v'(\rho + p_r)}{2}, \quad F_h = -\frac{dp_r}{dr}, \quad \& \quad F_a = \frac{2(p_t - p_r)}{r},$$

$$\& \quad F_e = -\frac{-\frac{1}{4}\beta\frac{dp_r}{dr} - \beta\frac{dp_t}{dr} + \frac{1}{4}\beta\frac{d\rho}{dr}}{\frac{\beta}{2} + 4\pi}. \quad (40)$$
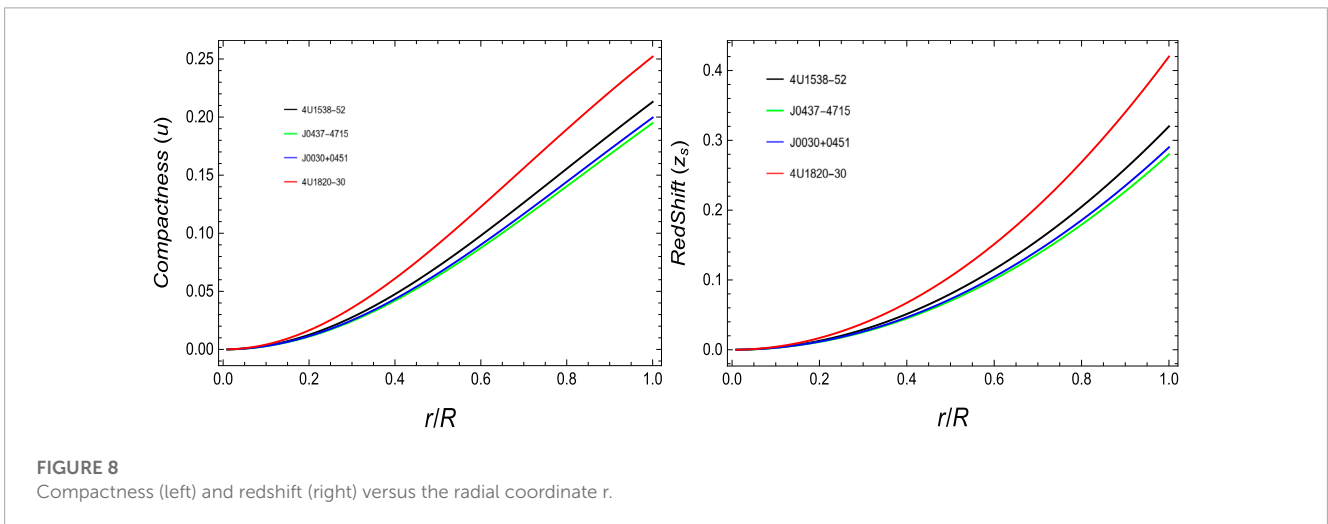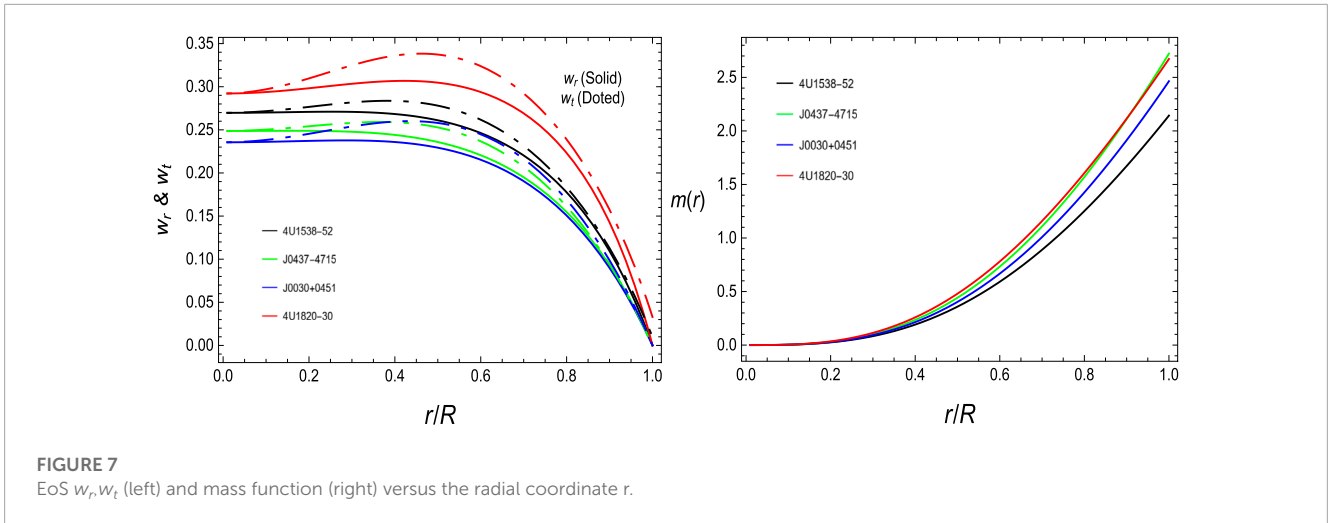
TOV forces define the stability of the system by escaping it to collapse to a singular point during the gravitational forces as these forces cancel each other's effect by giving the net impact equal to zero. The balancing behavior of TOV forces in our study is shown in the right graph of Figure 6.

5.7 Equation of state profiles w_r & w_t

The matter composition of the stellar body may be real or dark matter. It is very important to discuss the essence of matter composition. Limits on the components of EoS $0 \le w_r < 1, \& 0 < w_t < 1$ guarantee the real nature of matter composition. If the compact star is composed of realistic anisotropic matter, the obtained results will satisfy this stability criterion. Violation of the limits defined for EOS could potentially indicate the presence of exotic matter or dark matter. The expression for EoS is given as

$$w_r = \frac{p_r}{\rho} \quad \& \quad w_t = \frac{p_t}{\rho}. \quad (41)$$

One can easily be satisfied by the behavior of EoS parameter graphs, which are shown on the graph on the left of Figure 7, that our stellar system under study shows the realistic composition of matter.

FIGURE 7
EoS w_r, w_t (left) and mass function (right) versus the radial coordinate r.

FIGURE 8
Compactness (left) and redshift (right) versus the radial coordinate r.

5.8 Mass function redshift and compactness profiles

The ratio $\frac{m(r)}{R}$ defines the compactness level of the stellar system, where $m(r)$ is the mass function representing the total mass of the star, which can be evaluated by the following formula:

$$m(R) = 4\pi \int r^2 \rho dr. \tag{42}$$

Using (42), one can evaluate the compactness $u(r)$, which is given in Eq. 43, which is further used in the evaluation of the redshift function z_s in Eq. 44. $u(r) \& z_s$ are in the following equations:

$$u(r) = \frac{m(R)}{R}, \tag{43}$$

$$z_s = (1 - 2u)^{-\frac{1}{2}} - 1. \tag{44}$$

Bowers and Liang (1974) defined the peak limit for the compactness parameter as $u(r) = \frac{m(r)}{R} < \frac{4}{9}$. Andreasson (2008) generalized this limit for the anisotropic composition of matter. The maximum limit for the redshift parameter was set by Buchdahl (1959) as $z_s \le 4.77$. The regular behaviors of mass function, compactification, and redshift are plotted in the right graph of Figure 7 and Figure 8.

6 Conclusion

It is important to mention that the potential component of interior geometry is crucial in the study of stellar objects. In this study, we used the function $\lambda(r) = \left(\frac{cr^2}{R^2} + 1\right)^2$ as a defining function, which has been used in previous studies (Jamil et al., 2013; Sarma and Ratanpal, 2013; Solanki and Jackson Levi Said, 2022). However, in this study, it is the first time it is being coupled with trace and torsion. The role of c is critical in modeling the stellar structure. Additionally, the function $f(T, \mathcal{T}) = \alpha T^n(r) + \beta \mathcal{T}(r) + \phi$ is of primary importance and generalizes the study for a broader spectrum. We can retrieve the basic formalism of various modifications of gravities. For instance, $\alpha = n = 1$ and $\beta = \phi = 0$ lead us to the original teleparallel gravity, where $\alpha \ne 0, 1$ and $\beta = 0$ lead us to the $f(T)$ gravity. On the other hand, $\alpha \ne 0$ and $\beta \ne 0$ maintain the current form of coupling between trace and torsion. The degree of $f(T)$ modification is defined by integral values of n. By varying the values of n, one can check the stable degree of torsion modifications. According to our observations in the current analysis, $f(T, \mathcal{T})$ gravity is stable only for $n = 1 \& 2$ (Zubair et al., 2021). So, the model $f(T, \mathcal{T}) = \alpha T^n(r) + \beta \mathcal{T}(r) + \phi$ bears some stability limitations for $n \ge 3$ (Zubair et al., 2021). Thus,

as a whole, this study represents the most general form of gravity modifications.

This study comprises the study of the anisotropic nature of neutron star candidates $4U1538-52$, $J0437-4,715$, $J0030 + 0451$, and $4U1820-30$. In this study, we elaborate the properties of compact objects under the formalism of $f(T,\mathcal{T})$ gravity, which is composed of the matter term $\mathcal{T}$ coupling with torsion T by taking into account the off-diagonal tetrad. FEs are calculated by using the spherically symmetric space–time. The metric functions we chose for this were also studied by Solanki and Jackson Levi Said (2022) by using $f(T)$ gravity. However, they did not study the complete properties of compact objects, which we have discussed in this article, like the TOV equation, EoS components, the behavior of metric potentials, mass function, redshift, and compactification using the $f(T,\mathcal{T})$ gravity framework. Traditional junction conditions are used by matching the interior spherical and symmetric space–time with the exterior Schwarzschild space–time to evaluate the constant parameters whose simplified values are tabulated in Table 1. We conclude the discussion of our results as follows:

- Metric components $e^{\mu(r)} \& e^{\lambda(r)}$ show regular positive behavior, as shown in the left graph of Figure 1.
- Energy density ρ, plotted in right of Figure 1, has the physically acceptable positive conduct by showing a maximum value at the center and a minimum value at the boundary.
- Behavior of pressure profiles, as shown in Figure 2, is also up to the mark according to the study of compact objects of anisotropic nature with a maximum value at the center and a minimum value at the boundary.
- Gradients profiles justify the condition $\frac{d\rho}{dr}|_{(0<r\leq R)} \leq 0$, $\frac{dp_r}{dr}|_{(0<r\leq R)} \leq 0$, $\frac{dp_t}{dr}|_{(0<r\leq R)} \leq 0$ starting from zero to a negatively increasing value toward the boundary, as shown in the right graph of Figure 3, which show the compact formation of the stellar system.

The positive anisotropic repulsive force $\Delta \geq 0$ ensures the stability of the system by acting against the inward gravitational force. The left graph of Figure 3 shows the positive behavior of anisotropy Δ.

- Matter distribution of the stellar system is real, which is ensured by the positive energy limits, which are graphed in Figure 4. It can easily be verified that all the energy limits are positive all over the stellar structure, which means that the matter is real in nature without any existence of dark matter.
- Speeds of sound also ensure the stability of the system by obeying the cracking limits $0 < v_r^2 \& v_t^2 < 1$, i.e., there is no cracking in the system, as shown in Figure 5. Moreover, generalized stability criteria $0 < |v_t^2 - v_r^2| < 1$ are also fulfilled, as shown in the graph in the right of Figure 6.
- The system is stable without any point singularity, which is ensured by the balance of TOV forces which are graphed in the left graph of Figure 6. All the four forces, F_a, F_g, F_h and F_e, are in balance.
- EoS components w_r and w_t are plotted in the right graph of Figure 7. A graphical representation of these components denies the existence of dark matter by fulfilling the real matter distribution criteria $0 < w_r$ and $w_t < 1$.
- Regular and acceptable behaviors of the mass function, redshift, and compactification are plotted in the left of Figures 7, 8. It can be confirmed from the graphs that these parameters fulfill all the stability limits discussed in Subsection 8 of section V.

DittaAshraf et al. (2021), Zubair et al. (2021), Gudekli et al. (2022), and Zubair et al. (2022) studied the stellar models in $f(T,\mathcal{T})$ gravity. It is noticeable that the results in our case are less dense than those in the previous studies. Moreover, Nashed and Bamba (2022) also studied stellar properties, and their results are also denser than our results. If $\alpha = n = 1$ and $\beta = \phi = 0$, we recover the teleparallel gravity, which is equivalent to GR. Thus, our results are also in agreement with GR.

Based on the detailed discussion regarding the results, the overall conclusion can be strengthened that our discussed models of neutron stars are stable and show the overall reliability of compact object studies. In this article, we present the results of a study on the quadratic model of $f(T,\mathcal{T})$ gravity with $n = 2$. This model can be conveniently adapted to other modifications of $f(T)$ gravity. In future studies, we suggest comparing three forms of $f(T)$ gravity: $\alpha = n = 1$ and $\beta = \phi = 0$ for TEGR, $\alpha \neq 0$ and $\beta = 0$ for $f(T)$ gravity, and $\alpha \neq 0, \beta \neq 0$ for $f(T,\mathcal{T})$ gravity. By comparing the results, we can identify the main effects of these gravity modifications. This comparison can also be extended to higher-order models, such as $n \geq 3$. Overall, the results of this study are interesting and could be beneficial for future research in this field.

Data availability statement

The original contributions presented in the study are included in the article/Supplementary Material, further inquiries can be directed to the corresponding author.

Author contributions

All authors listed have made a substantial, direct, and intellectual contribution to the work and approved it for publication.

Acknowledgments

Conflict of interest

The authors declare that the research was conducted in the absence of any commercial or financial relationships that could be construed as a potential conflict of interest.

Publisher's note

All claims expressed in this article are solely those of the authors and do not necessarily represent those of their affiliated organizations, or those of the publisher, the editors, and the reviewers. Any product that may be evaluated in this article, or claim that may be made by its manufacturer, is not guaranteed or endorsed by the publisher.

References

Abbas, G., and Nazar, H. (2021). Ann. *Phys.* 424, 168336.

Abbas, G., and Nazar, H. (2018). Complexity factor for anisotropic source in non-minimal coupling metric f(R) gravity. *Eur. Phys. J. C* 78, 957. doi:10.1140/epjc/s10052-018-6430-8

Abreu, H., Hernandez, H., and Nunez, L. A. (2007). Sound speeds, cracking and the stability of self-gravitating anisotropic compact objects. *Calss. Quantum. Grav.* 24, 4631–4645. doi:10.1088/0264-9381/24/18/005

Aldrovandi, R., and Pereira, J. G. (2012). *Teleparallel gravity: An introduction*. Dordrecht: Springer.

Andreasson, H., *J. Diff. Eq.* 245, 2243 (2008).

Bamba, K., Capozziello, S., Nojiri, S., and Odintsov, S. D. (2012a). Dark energy cosmology: the equivalent description via different theoretical models and cosmography tests. *Astrophys. Space Sci.* 345, 155–228. doi:10.1007/s10509-012-1181-8

Behar, S., and Carmeli, M. (2000). *Intern. J. Theor. Phys.* 39, 1375–1396. doi:10.1023/a:1003651222960

Boehmer, C. G., Mussa, A., and Tamani, S. (2011). *Cl. Quantum Gravity* 28, 245020.

Bowers, R. L., and Liang, E. P. T. (1974). Anisotropic spheres in general relativity. *Cl. Astrophys. J.* 188, 657. doi:10.1086/152760

Buchdahl, H. A. (1959). General relativistic fluid spheres. *Phys. Rev. D.* 116, 1027–1034. doi:10.1103/physrev.116.1027

Camera, S., Cardone, V. F., and Radicella, N. (2014). Detectability of torsion gravity via galaxy clustering and cosmic shear measurements. *Phys. Rev. D.* 89, 083520. doi:10.1103/physrevd.89.083520

Capozziello, S., and De Laurentis, M. (2011). Extended theories of gravity. *Phys. Rept.* 509, 167–321. doi:10.1016/j.physrep.2011.09.003

Cardone, V. F., Radicella, N., and Camera, S. (2012). Acceleratingf(T)gravity models constrained by recent cosmological data. *Phys. Rev. D.* 85, 124007. doi:10.1103/physrevd.85.124007

Carmeli, M., and Kuzmenko, T. (2001), *Value of the Cosmological Constant: Theory versus Experiment*, arXiv: astro-ph/0102033.

Clifton, T., Ferreira, P. G., Padilla, A., and Skordis, C. (2012). Modified gravity and cosmology. *Phys. Rept.* 513, 1–189. doi:10.1016/j.physrep.2012.01.001

Deb, D., et al. (2019). Mon. Notices royal astron. *Soc.* 485, 5652.

Dent, J. B., Duuta, S., and Saridakis, E. N. (2011). $f(T)$ gravity mimicking dynamical dark energy. Background and perturbation analysis. *J. Cosmol. Astropart. Phys.* 1101, 009. doi:10.1088/1475-7516/2011/01/009

Ditta, A., Hussain, I., Mustafa, G., Errehymy, A., and Daoud, M. (2021). A study of traversable wormhole solutions in extended teleparallel theory of gravity with matter coupling. *Eur. Phys. J. C* 81, 880. doi:10.1140/epjc/s10052-021-09668-7

DittaAshraf, A. A., Zhang, Z., and Mustafa, G. (2021). Modeling of anisotropic spheres in extended teleparallel theory with matter coupling. *Chin. J. Phys.* 69, 240–252. doi:10.1016/j.cjph.2020.11.025

Einstein, A., and Preuss, S. B. (1925). Akad. *Wiss.* 22, 414.

Famaey, B., and McGaugh, S. (2012). Modified Newtonian dynamics (MOND): observational phenomenology and relativistic extensions. *Living Rev. rel.* 15, 10. doi:10.12942/lrr-2012-10

Ferraro, R., and Fiorini, F. (2008). Born-Infeld gravity in Weitzenböck spacetime. *Phys. Rev. D.* 78, 124019. doi:10.1103/physrevd.78.124019

Fiorini, F., and Ferraro, R. (2009). *Int. J. Mod. Phys. A* 24, 1686–1689. doi:10.1142/s0217751x09045236

Gudekli, E., KamranZubair, M. J. M., and Ahmed, I. (2022). Study of anisotropic strange stars in Krori Barua metric under f(T,T) gravity. *Chin. J. Phys.* 77, 592–604. doi:10.1016/j.cjph.2021.08.006

Harko, T., et al. (2014). *J. Cosmol. Astropart. Phys.* 12 (021). ar Xiv:1405.0519v3 [gr-qc].

Herrera, L. (1992). Cracking of self-gravitating compact objects. *Phys. Lett. A* 165, 206–210. doi:10.1016/0375-9601(92)90036-l

Herrera, L., and Santos, N. O. (1997). Local anisotropy in self-gravitating systems. *Phys. Rep.* 286, 53–130. doi:10.1016/s0370-1573(96)00042-7

Iorio, L., and Saridakis, E. N. (2012a). Solar system constraints on$f(T)$ gravity: solar system constraints on$f(T)$ gravity. *Mon. Not. R. Astron. Soc.* 427, 1555–1561. doi:10.1111/j.1365-2966.2012.21995.x

Ivanov, B. V. (2002). Maximum bounds on the surface redshift of anisotropic stars. *Phys. Rev. D.* 65, 104011. doi:10.1103/physrevd.65.104011

Jamil, M., Momeni, D., and Myrzakulov, R. (2013). Wormholes in a viable f(T) gravity. *Eur. Phys. J. C* 73 (1), 2267. doi:10.1140/epjc/s10052-012-2267-8

Jeans, J. (1922). The motions of stars in a kapteyn-universe. *Mon. Not. R. Astron. Soc.* 82, 122–132. doi:10.1093/mnras/82.3.122

Li, B., Sotiriou, T. P., and Barrow, J. D. (2011). f(T)gravity and local Lorentz invariance. *Phys. Rev. D.* 83, 064035. doi:10.1103/physrevd.83.064035

Mak, M. K., and Harko, T. (2002). An exact anisotropic quark star model. *Chin. J. Astron. Astrophys.* 2, 248–259. doi:10.1088/1009-9271/2/3/248

Maurya, S. K., Gupta, Y. K., Ray, S., and Deb, D. (2016). Generalised model for anisotropic compact stars. *Eur. Phys. J. C* 76, 693. doi:10.1140/epjc/s10052-016-4527-5

Maurya, S. K., Errehymy, A., Deb, D., Tello-Ortiz, F., and Daoud, M. (2019). Study of anisotropic strange stars in f (R, T) gravity: An embedding approach under the simplest linear functional of the matter-geometry coupling. *Phys. Rev. D.* 100 (4), 044014. doi:10.1103/physrevd.100.044014

Maurya, S. K., Mustafa, G., Govender, M., and Singh, K. N. (2022). Exploring physical properties of minimally deformed strange star model and constraints on maximum mass limit in f (𝒬) gravity. *J. Cosmol. Astropart. Phys.* 2022 (10), 003. doi:10.1088/1475-7516/2022/10/003

Mustafa, G., Shamir, M. F., and Tie-Cheng, X. (2020). Physically viable solutions of anisotropic spheres in f (R, G) gravity satisfying the Karmarkar condition. *Phys. Rev. D.* 101 (10), 104013. doi:10.1103/physrevd.101.104013

Mustafa, G., Ahmad, M., Ali, Ö., Shamir, M. F., and Hussain., I. (2021). Traversable wormholes in the extended teleparallel theory of gravity with matter coupling. *Fortschritte Phys.* 69, 8–9.

Mustafa, G., Gao, X., and Javed, F. (2022a). Twin peak quasi-periodic oscillations and stability via thin-shell formalism of traversable wormholes in symmetric teleparallel gravity. *Fortschritte Phys.* 70 (9-10), 2200053. doi:10.1002/prop.2022 00053

Mustafa, G., Maurya, S. K., and Ray, S. (2022b). On the possibility of generalized wormhole formation in the galactic halo due to dark matter using the observational data within the matter coupling gravity formalism. *Astrophysical J.* 941 (2), 170. doi:10.3847/1538-4357/ac9b00

Mustafa, G., Maurya, S. K., and Hussain, I. (2023). Relativistic wormholes in extended teleparallel gravity with minimal matter coupling. *Fortschritte Phys.* 71 (4-5), 2200119. doi:10.1002/prop.202200119

Nashed, G. G. L., and Bamba, K. (2022). *Prog. Theor. Exp. Phys.* 2022, 23.

Nazar, H., and Abbas, G. (2021). Advan. *Astron.* 2021, 6698208.

Nazar, H., et al. (2021). *Int. J. Mod. Phys. A* 36, Nos. 31&32, 2150233.

Nojiri, S., and Odintsov, S. D. (2007). *Int. J. Geom. Meth.Mod. Phys.* 4, 115–145. doi:10.1142/s0219887807001928

Oppenheimer, J. R., and Volkoff, G. M. (1939). On massive neutron cores. *Phys. Rev.* 55, 374–381. doi:10.1103/physrev.55.374

Pace, M., and Said, J. L (2017). Quark stars in $f(T, \mathcal{T})$ f (T, T) -gravity. *Eur. Phys. J. C* 77, 62. doi:10.1140/epjc/s10052-017-4637-8

Rahaman, M., Singh, Ksh. N., Errehymy, A., Rahaman, F., and Daoud, M. (2020). Anisotropic Karmarkar stars in f(R, T)-gravity. *Eur. Phys. J. C* 80, 272. doi:10.1140/epjc/s10052-020-7842-9

Riess, A. G., et al. (1998). (Supernova search team collaboration). *Astron. J.* 116, 1009.

Ruderman, R. (1972). Pulsars: structure and dynamics. *Rev. Astron. Astrophys.* 10, 427–476. doi:10.1146/annurev.aa.10.090172.002235

Salako, I. G., Khlopov, M., Ray, S., and Arouko, M. Z. (2020). *Pameli saha*. China: Ujjal Debnath. arXiv:2004.07959 [gr-qc].

Sarma, R., and Ratanpal, B. S. (2013). *Int. J. Mod. Phys. D.* 22, 1350074. doi:10.1142/s0218271813500740

Sawyer, R. F. (1972). Condensedπ−Phase in neutron-star matter. *Phys. Rev. Lett.* 29, 382–385. doi:10.1103/physrevlett.29.382

Singh, K. N., Maurya, S., Errehymy, A., Rahaman, F., and Daoud, M. (2020). Physical properties of class I compact star model for linear and Starobinsky–f(R,T) functions. *Phys. Dark Universe* 30, 100620. doi:10.1016/j.dark.2020.100620

Sokolov, A. I. (1980). *J. Exp. Theor. Phys.* 79, 1137.

Solanki, Jay, and Jackson Levi Said (2022). Anisotropic stellar model of neutron stars in f(T) gravity with off-diagonal tetrad. *Eur. Phys. J. C* 82, 35. doi:10.1140/epjc/s10052-022-09995-3

Sotiriou, T. P., and Faraoni, R. (2010). f(R)theories of gravity. *Rev. Mod. Phys.* 82, 451–497. doi:10.1103/revmodphys.82.451

Tamanini, N., and Boehmer, G. C. (2012). Good and bad tetrads inf(T)gravity. *Phys. Rev. D.* 86, 044009. doi:10.1103/physrevd.86.044009

Tolman, R. C. (1939). Static solutions of einstein's field equations for spheres of fluid. *Phys. Rev.* 55, 364–373. doi:10.1103/physrev.55.364

Waheed, S., Mustafa, G., Zubair, M., and Ashraf, A. (2020). Physically acceptable embedded class-I compact stars in modified gravity with karmarkar condition. *Symmetry* 12, 962. doi:10.3390/sym12060962

Will, C. F. (2006). The confrontation between general relativity and experiment. *Living Rev. Relativ.* 9, 3. doi:10.12942/lrr-2006-3

Xie, Y., and Deng, X. M. (2013a). f(T) gravity: effects on astronomical observations and Solar system experiments and upper bounds. *Mon. Not. R. Astron. Soc.* 433, 3584–3589. doi:10.1093/mnras/stt991

Zubair, M., and Abbas, G. (2016). Analytic models of anisotropic strange stars in f (T) $f(T)$ gravity with off-diagonal tetrad. *Astrophys. Space Sci.* 361, 27. doi:10.1007/s10509-015-2610-2

Zubair, M., Abbas, G., and Noureen, I. (2016). Possible formation of compact stars in f (R, T) $f(R,T)$ gravity. *Astrophys. Space Sci.* 361, 8. doi:10.1007/s10509-015-2596-9

Zubair, M., Ditta, A., Waheed, S., and Tello-Ortiz, F. (2022). Class I stars in the background of f(T,τ) cosmological model. *Chin. J. Phys.* 77, 1827–1842. doi:10.1016/j.cjph.2021.12.029

Zubair, M., Ditta, A., Abbas, G., and Saleem, R., *Chinese physics C* 45, 8 (2021).

Appendix A

$$l_1(r) = \sqrt{\frac{(cr^2 + R^2)^2}{R^4}}, \quad l_2(r) = \sqrt{\left(\frac{cr^2}{R^2} + 1\right)^2},$$

$$l_3(r) = \left(\frac{(l_2(r) - 1)\left(-\frac{r^6 z + r^4 R^2 y + r^2 R^4 x}{cr^2 R^4 + R^6} + l_2(r) - 1\right)}{\left(\frac{cr^3}{R^2} + r\right)^2}\right)^{n-1},$$

$$l_4(r) = \left(\frac{(l_2(r) - 1)\left(-\frac{r^6 z + r^4 R^2 y + r^2 R^4 x}{cr^2 R^4 + R^6} + l_2(r) - 1\right)}{\left(\frac{cr^3}{R^2} + r\right)^2}\right)^{n},$$

$$l_5(r) = \left(\frac{(l_1(r) - 1)\left(-\frac{r^6 z + r^4 R^2 y + r^2 R^4 x}{cr^2 R^4 + R^6} + l_2(r) - 1\right)}{\left(\frac{cr^3}{R^2} + r\right)^2}\right)^{n}.$$